ITEP-LAT/2011-14

Lattice Gluon Propagators in $3d$ $SU(2)$ Theory and Effects of Gribov Copies

V. G. Bornyakov
Institute for High Energy Physics, 142281, Protvino, Russia
and Institute of Theoretical and Experimental Physics, 117259 Moscow, Russia

V. K. Mitrjushkin
Joint Institute for Nuclear Research, 141980 Dubna, Russia
and Institute of Theoretical and Experimental Physics, 117259 Moscow, Russia

R. N. Rogalyov
Institute for High Energy Physics, 142281, Protvino, Russia
(Dated: 25.06.2012)

Infrared behavior of the Landau gauge gluon propagators is studied numerically in the 3d $SU(2)$ gauge theory on the lattice. A special accent is made on the study of Gribov copy effect. For this study we employ an efficient gauge-fixing algorithm and a large number of gauge copies (up to 280 copies per configuration). It is shown that, in the deep infrared region, the Gribov copy effects are very significant. Also we show that, in the infinite-volume limit, the zero-momentum value of the propagator does not vanish.

PACS numbers: 11.15.Ha, 12.38.Gc, 12.38.Aw
Keywords: Lattice gauge theory, gluon propagator, Gribov problem, simulated annealing

I. INTRODUCTION

The nonperturbative (first principle) numerical computation of the field propagators is important for various reasons. There are scenarios of confinement based on infrared behavior of the gauge dependent propagators. In particular, in the Gribov-Zwanziger (GZ) confinement scenario [1, 2] the Landau-gauge gluon propagator $D(p)$ at infinite volume is expected to vanish in the infrared (IR) limit $p \to 0$. On the other hand, a refined Gribov-Zwanziger (RGZ) scenario proposed recently [3–5] allows a finite nonzero value of $D(0)$. Another reason is that the nonpertubative lattice calculations are necessary to check the results obtained by analytical methods, e.g., the Dyson-Schwinger equations (DSE) approach which uses truncations of the infinite set of equations. The DSE scaling solution predicts that the propagator tends to zero in the zero-momentum limit [6, 7] in accordance with the RGZ-scenario. At the same time, the DSE decoupling solution [8–11] allows a finite nonzero value of $D(0)$ in conformity with RGZ-scenario.

The $3d$ $SU(2)$ theory can serve as a useful testground to verify these predictions in a simplified, in comparison with the $4d$ case, setting. Furthermore, $3d$ theory is of interest for the studies of the high-temperature limit of the $4d$ theory.

The most theoretically attractive definition of the Landau gauge is to choose for every gauge orbit a representative from the fundamental modular region [12], i.e. the *absolute* maximum of the gauge fixing functional $F(U)$ (see the definition in Section II.).

The arguments in favor of this choice are the following : **a)** a consistent non-perturbative gauge fixing procedure proposed by Parrinello–Jona-Lasinio and Zwanziger (PJLZ-approach) [13, 14] presumes that the choice of a unique representative of the gauge orbit should be through the *global* extremum of the chosen gauge fixing functional; **b)** in the case of pure gauge $U(1)$ theory in the weak coupling (Coulomb) phase some of the gauge copies produce a photon propagator with a decay behavior inconsistent with the expected zero mass behavior [15–17]. The choice of the global extremum permits to obtain the physical - massless - photon propagator. It should be noted that, for practical purposes, it is sufficient to approach the global maximum close enough so that the systematic errors due to nonideal gauge fixing (because of, e.g., Gribov copy effects) are of the same magnitude as statistical errors. We follow here this strategy which has been checked already in many papers on $4d$ theory studies for both $SU(2)$ [18–22] and $SU(3)$ [19, 23–25] gauge groups.

The three-dimensional $SU(2)$ theory has been recently studied in [26–31]. The evidence has been presented that the propagator has a maximum at momenta about 350 MeV and that $D(0)$ does not converge to zero in the infinite-volume limit. The problem of Gribov-copy effects was addressed in [30]. The Gribov-copy effects for the gluon propagator were found for small momenta. We will show in this paper that these effects were underestimated.

As compared to the previous version of this article, we take into account the lattices 80^3 and 96^3 and obtain better statistics on lattices of smaller size. For this reason, we make the respective improvements in our plots, and draw more definite conclusions.

In Section II we introduce the quantities to be computed. In Section III some details of our simulations are given. In Section IV we discuss the effect of im-

proved gauge fixing and present our numerical results. Conclusions are drawn in Section V.

II. THE GLUON PROPAGATOR: DEFINITIONS

We consider cubic $L \times L \times L$ lattice Λ with spacing a. To generate Monte Carlo ensembles of thermalized configurations we use the standard Wilson action

$$S = \beta \sum_{x,\mu>\nu} \left[1 - \frac{1}{2} \ \mathrm{Tr}\Big(U_{x\mu} U_{x+\hat{\mu};\nu} U^{\dagger}_{x+\hat{\nu};\mu} U^{\dagger}_{x\nu} \Big) \right] , \tag{1}$$

where $\beta = 4/g^2 a$, $\hat{\mu}$ is a vector of length a along the μth coordinate axis and g denotes dimensionful bare coupling. $U_{x\mu} \in SU(2)$ are the link variables which transform under local gauge transformations g_x as follows:

$$U_{x\mu} \stackrel{g}{\mapsto} U^g_{x\mu} = g^{\dagger}_x U_{x\mu} g_{x+\hat{\mu}} \, , \qquad g_x \in SU(2) \, . \tag{2}$$

We study the gluon propagator

$$D^{bc}_{\mu\nu}(q) = \frac{a^3}{L^3} \sum_{x,y \in \Lambda} \exp(iqx) \langle A^b_{\mu}(x+y) A^c_{\nu}(y) \rangle, \tag{3}$$

where the vector potentials are defined as follows [32]:

$$A_{\mu} \equiv \sum_{b=1}^{3} A^b_{\mu} \frac{\sigma^b}{2} = \frac{i}{ga} \big(U_{x,\mu} - U^{\dagger}_{x,\mu} \big), \tag{4}$$

and the momenta q_μ take the values $q_\mu = 2\pi n_\mu / aL$, where n_μ runs over integers in the range $-L/2 \leq n_\mu < L/2$. The gluon propagator can be represented in the form

$$D^{bc}_{\mu\nu}(q) = \begin{cases} \delta^{bc} \delta_{\mu\nu} \bar{D}(0), & p = 0; \\ \delta^{bc} \left(\delta_{\mu\nu} - \dfrac{p_\mu p_\nu}{p^2} \right) \bar{D}(p), & p \neq 0, \end{cases}$$

where $p_\mu = \dfrac{2}{a} \sin \dfrac{q_\mu a}{2}$ and $p^2 = \sum_{\mu=1}^{3} p^2_\mu$. When $p \neq 0$, we arrive at

$$\bar{D}(p) = \beta \frac{a^2}{3} \ \frac{1}{2L^3} \ \sum_{\mu=1}^{3} \sum_{b=1}^{3} \langle c^b_\mu(q) c^b_\mu(q) + s^b_\mu(q) s^b_\mu(q) \rangle, \tag{5}$$

where

$$\begin{aligned} c^b_\mu(q) \ &= \ \sum_{x \in \Lambda} \cos(qx) \ u^b_\mu(x), \\ s^b_\mu(q) \ &= \ \sum_{x \in \Lambda} \sin(qx) \ u^b_\mu(x), \end{aligned} \tag{6}$$

and $u^b_\mu = -gaA^b_\mu/2$. For zero-momentum propagator one obtains

$$\bar{D}(0) = \frac{\beta \, a^2}{9 \, L^3} \ \sum_{\mu=1}^{3} \sum_{b=1}^{3} \langle c^b_\mu(0) c^b_\mu(0) \rangle. \tag{7}$$

In the weak-coupling infinite-volume limit, $\bar{D}(p) = \dfrac{1}{p^2}$. In this work, we deal with the quantity (referred to as the gluon propagator) [1]

$$D(p) = \bar{D}(p)/\beta; \tag{8}$$

In lattice gauge theory the usual choice of the Landau gauge condition is [32]

$$(\partial A)(x) = \frac{1}{a} \ \sum_{\mu=1}^{3} \left(A_\mu(x) - A_\mu(x - \hat{\mu}) \right) = 0 \, , \tag{9}$$

which is equivalent to finding a local extremum of the gauge functional

$$F_U(g) = \ \frac{1}{3L^3} \sum_{x\mu} \ \frac{1}{2} \ \mathrm{Tr} \ U^g_{x\mu} \tag{10}$$

with respect to gauge transformations g_x. The manifold consisting of Gribov copies providing local maxima of the functional (10) and a semi-positive Faddeev-Popov operator is termed the *Gribov region* Ω, while that of the global maxima is termed the *fundamental modular region* (FMR) $\Gamma \subset \Omega$. Our gauge-fixing procedure is aimed to approach Γ.

III. DETAILS OF THE SIMULATION

In this work, we are going to demonstrate that the gluon propagator in the deep infrared region can be reliably evaluated only when the effects of Gribov copies are properly taken into account. We make simulations at a fixed gauge coupling on various lattices using gauge-fixing algorithm which was already successfully employed in the $4d$ theory at both zero [20, 21] and nonzero [22, 25] temperature. There are three main ingredients of this algorithm: powerful simulated annealing algorithm, which proved to be efficient in solving various optimization problems; the flip transformation of gauge fields, which was used to decrease both the Gribov-copy and finite-volume effects [20–22]; simulation of a large number of gauge copies for

[1] Note that the function $\bar{D}(p)$ (not $D(p)$!) is normalized similar to the analogous function used in [28] and [30].

each flip sector in order to further decrease the effects of Gribov copies.

We perform Monte Carlo (MC) simulations at $\beta = 4.24$ for various lattice sizes L. Consecutive configurations (considered to be statistically independent) were separated by 200 sweeps, each sweep consisting of one local heatbath update followed by 15 microcanonical updates. In Table I we provide the full information about the field ensembles used in this investigation.

L	n_{meas}	n_{copy}	aL[fm]	p_{min}[GeV]
32	800	96	5.38	0.230
36	1037	160	6.05	0.204
40	1032	160	6.73	0.184
44	717	160	7.39	0.167
48	1425	160	8.08	0.153
52	1085	160	8.74	0.141
56	796	160	9.43	0.131
64	709	160	10.8	0.115
72	910	280	12.1	0.102
80	557	160	13.5	0.092
96	438	280	16.1	0.077

TABLE I: Values of lattice size, L, number of measurements n_{meas} and number of gauge copies n_{copy} used throughout this paper. Spacing is $a = 0.168$ fm.

The features of the gauge-fixing methods [19] used in our study are as follows. Firstly, we extend the gauge group by the transformations (also referred to as Z_2 flips) defined as follows:

$$f_\nu(U_{x,\mu}) = \begin{cases} -U_{x,\mu} & \text{if} \quad \mu = \nu \quad \text{and} \quad x_\mu = a, \\ U_{x,\mu} & \text{otherwise} \end{cases}$$

which are the generators of the Z_2^3 group leaving the action (1) invariant.

Such flips are equivalent to nonperiodic gauge transformations. A Polyakov loop directed along the transformed links and averaged over the 2-dimensional plane changes its sign. Therefore, the flip operations combine the 2^3 distinct gauge orbits (or Polyakov loop sectors) of strictly periodic gauge transformations into one larger gauge orbit.

The second feature is making use of the simulated annealing (SA), which has been found computationally more efficient than the use of the standard overrelaxation (OR) only [19, 33, 34]. The SA algorithm generates gauge transformations $g(x)$ by MC iterations with a statistical weight proportional to $\exp\left(3V\, F_U[g]/T\right)$. The "temperature" T is an auxiliary parameter which is gradually decreased in order to maximize the gauge functional $F_U[g]$. In the beginning, T has to be chosen sufficiently large in order to allow traversing the configuration space of $g(x)$ fields in large steps. As in Ref. [19], we choose $T_{\rm init} = 1.5$. After each quasi-equilibrium sweep, including both heatbath and microcanonical updates, T is decreased with equal step size. The final SA temperature is fixed such that during the consecutively applied OR algorithm the violation of the transversality condition

$$\max_{x,\,a} \left| \sum_{\mu=1}^{3} \left(u^a_\mu(x) - u^a_\mu(x-\hat{\mu}) \right) \right| < \epsilon \qquad (11)$$

decreases in a more or less monotonous manner for the majority of gauge fixing trials until the condition (11) becomes satisfied with $\epsilon = 10^{-7}$. A monotonous OR behavior is reasonably satisfied for a final lower SA temperature value $T_{\rm final} = 0.01$ [33]. The number of temperature steps is set equal to 3000. The finalizing OR algorithm using the standard Los Alamos type overrelaxation with the parameter value $\omega = 1.7$ requires typically a number of iterations of the order $O(10^3)$.

We then take the best copy out of many gauge fixed copies obtained for the given gauge field configuration, i.e., a copy with the maximal value of the lattice gauge fixing functional F as a best estimator of the *global* extremum of this functional.

In what follows, we consider three gauge-fixing methods.

The first employs both the SA-OR algorithm and the Z_2 flips. Using the SA-OR algorithm, we generate $8n_c$ Gribov copies (n_c copies in each Z_2^3 sector) and find the copy giving the maximum of the functional (10). This copy is referred to as the best copy ("*bc*") and it should be mentioned that we also find "the best sector" for each starting configuration. The version of the Landau gauge obtained by this method is labelled FSA ("Flipped Simulated Annealing").

The second method employs the SA-OR algorithm, whereas the Z_2 flips are not taken into consideration. In this case, we choose "the best copy" from n_c configurations, that corresponds to a random choice of the Z_2^3 sector. We name it "SA gauge-fixing" (it is analogous in some sense to the "absolute gauge fixing" in [30]).

In order to demonstrate the effect of Gribov copies, we also consider the gauge obtained by a random choice of a copy within the first Gribov horizon (labelled as "*fc*"—first copy). That is, in the third case, we take the first copy obtained by the SA algorithm and do not take care of fundamental modular domain at all. This version of the Landau gauge is analogous in some sense to the "minimal Landau gauge" in [30]).

Information on our simulation procedure is also shown in Table I. The scale is set by the relation $a\sqrt{\sigma} \approx 0.376$ for $\beta = 4.24$ (see formula (65) in [35]), where $\sigma \approx (440\ \text{MeV})^2$ is the string tension (which is assumed the same as in the four dimensions).

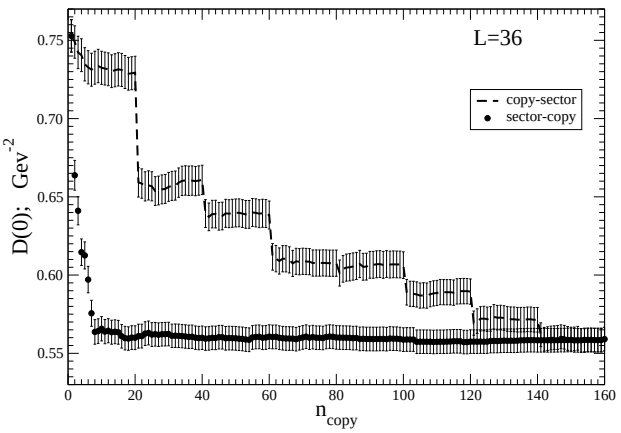

FIG. 1: $D(0)$ as a function of n_{copy}. The meaning of 'copy-sector' and 'sector-copy' is explained in the text.

IV. GRIBOV COPY EFFECTS AND LARGE L BEHAVIOR OF $D(0)$

To demonstrate the Gribov copy effects, we show in Fig. 1 the dependence of $D(0)$ on the number of gauge copies n_{copy} for $L = 36$ lattice. As one can see, the Gribov copy influence is very strong (at least, for $p = 0$), and by no means can be considered as a "Gribov noise".

For the upper curve in this Figure ('copy-sector') first 20 gauge copies belong to the first flip-sector, next 20 gauge copies belong to the second flip-sector, etc.. Evidently, the dependence on the number of copies belonging to the same flip-sector is rather weak (apart from the first one), and the main Gribov copy effect comes from different flip-sectors. This is demonstrated also by the lower curve ('sector-copy') where we have used another enumeration of gauge copies, i.e., $n_{copy} = 1$ corresponds to the 1st copy of the 1st flip-sector, $n_{copy} = 2$ means that first copies of the first and second flip-sectors are considered, etc.. With increasing volume $n_{copy}-$ dependence is changing as we will explain below in discussion of Fig. 3.

To compare Gribov copy effects for different values of L and $p \neq 0$, we define the Gribov copy sensitivity parameter $\Delta(p) \equiv \Delta(p; L)$ as a normalized difference of the *fc* and *bc* gluon propagators

$$\Delta(p) = \frac{D^{fc}(p) - D^{bc}(p)}{D^{bc}(p)} \ , \qquad (12)$$

where the numerator is the average of the differences between *fc* and *bc* propagators calculated for every configuration and normalized with the *bc* (averaged) propagator.

In Table II we show the values of the parameter $\Delta(p)$ for different values of L and four momenta : $p = 0$, p_{min}, $\sqrt{2}\,p_{min}$ and $\sqrt{3}\,p_{min}$. It is interesting to note that values of this parameter do *not* demonstrate the tendency to decreasing with increasing lattice size L for all momenta under consideration. In particular, at zero momentum the Gribov copy effect is estimated to be between appr. 25% and 35% (taking into account the error bars) for all values of L.

L	$p = 0$	p_{min}	$\sqrt{2}\,p_{min}$	$\sqrt{3}\,p_{min}$
32	0.318(14)	0.107(7)	0.043(5)	0.014(6)
36	0.329(13)	0.107(6)	0.039(4)	0.013(6)
40	0.289(13)	0.104(7)	0.039(5)	0.031(6)
44	0.308(16)	0.100(8)	0.042(5)	0.026(7)
48	0.251(11)	0.100(5)	0.046(4)	0.029(5)
52	0.285(13)	0.091(6)	0.043(4)	0.031(6)
56	0.273(15)	0.116(8)	0.042(5)	0.023(7)
64	0.294(17)	0.100(8)	0.049(6)	0.027(8)
72	0.261(16)	0.121(7)	0.052(5)	0.044(6)
80	0.232(20)	0.102(10)	0.062(7)	0.031(8)
96	0.218(21)	0.115(12)	0.074(8)	0.055(9)

TABLE II: Values of $\Delta(p)$ for the FSA Landau gauge propagators at $p = 0$, $p = p_{min}$, $p = \sqrt{2}\,p_{min}$ and $p = \sqrt{3}\,p_{min}$.

Therewith, for a given value of L, the parameter $\Delta(p)$ decreases quickly with an increase of the momentum. This observation is in agreement with the observations made earlier for the four-dimensional $SU(2)$ theory [21].

We have attempted to estimate the infinite-volume limit of the zero-momentum propagator $D(0; L)$, i.e., the limit $L \to \infty$.

One can apply various fit-formulas for this purpose, e.g., $c_1 + c_2/L$; c_2/L^{c_3}; $c_1 + c_2/L^{c_3}$, etc., and many of them fit nicely *if* the values of L are not very large (as in our case). However, calculations [28] on the lattice with $L = 320$ and $\beta = 3.0$ have shown that the first fit-formula is supposed to be the preferable one (at least, in the minimal Landau gauge). Therefore, following [28] we apply the fit-formula

$$D(0; L) = c_1 + c_2/L \qquad (13)$$

to determine the $L \to \infty$ limit of $D(0; L)$.

In Fig. 2 we show our values of $D(0; L)$ calculated for a) *fc* (which is the same for SA and FSA methods); b) *bc* SA method (i.e., without flips) and c) *bc* FSA method. Broken lines represent fits according to Eq. (13).

We confirm that in the $L \to \infty$ limit the value of $D(0)$ *differs* from zero. This is in agreement with the statement made in [28] and is not in conformity with [36] and [30].

Fig. 2 shows another interesting phenomenon : the Gribov copy influence survives even in the thermodynamic limit $L \to \infty$. Indeed, the infinite volume-extrapolation of $D^{fc}(0)$ *differs* from infinite-volume extrapolation of $D^{bc}(0)$ (both for SA and FSA gauge fixing algorithms).

To illustrate this phenomenon in a more explicit way, we calculated also the averaged (over all configurations) difference between *fc* and *bc* propagators normalized to $D^{bc}(p; L = \infty)$ (in what follows it will be refered to as $W(p)$). In Fig. 3 we show the dependence of $W(0)$ on the inverse lattice size both for SA and FSA algorithms. One can see that both algorithms predict *nonzero* difference between *fc* and *bc* values of the propagators, this difference being rather big ($\sim$ 15%) even in the thermodynamic limit. Note that both SA and FSA algorithms give the coincident (within errorbars) results in the $L \to \infty$ limit.

For small volumes $W(0)$ for SA algorithm, $W_{SA}(0)$, is close to zero while $W_{FSA}(0)$ is at its maximum. This corresponds to strong effects of flip-sectors seen in Fig. 1. With increasing volume $W_{SA}(0)$ is increasing indicating the increasing role of the copies within given flip-sector. In opposite, decreasing of $W_{FSA}(0)$ with increasing volume implies that the role of the flip-sectors reduces. In the infinite volume limit the two curves in Fig. 3 converge. This means that in this limit one randomly chosen flip-sector is sufficient or, in other words, all flip sectors are equivalent. Note that on our largest volume the effect of the flip-sectors is still dominating over the effect of the copies within one sector.

In Fig. 4 we compare the L-dependence of $W(0)$ shown in the previous Figure with that for two nonzero values of momenta: $|p| = 150$ MeV and $|p| = 250$ MeV (all calculated for FSA). The respective values of the propagators for fixed physical momenta were obtained by interpolation of the original data to necessary value of momentum. As it was expected, Gribov copy effects decrease quickly with increasing $|p|$. However, they are expected to be *not* small in the deep infrared region, i.e., in the $|p| \to 0$ limit. This can be essential for the calculation of, say, screening masses in $4d$ theory at nonzero temperature where the IR-behavior of the gluon propagator is important.

In Fig. 5 we compare the momentum dependence of the propagators $D(p)$ calculated on 36^3, 72^3 and 96^3 lattices. Qualitatively its momentum dependence agrees with that obtained earlier [30, 31, 37]. But in contrast to these papers the finite-volume effects are very small and can safely be neglected at momenta $p > 0.4$ GeV. Note that the propagator has a maximum at nonzero value of momentum $|p| \sim 400$ **MeV.** Therefore, the behavior of $D(p)$ in the deep infrared region is inconsistent with a simple pole-type dependence.

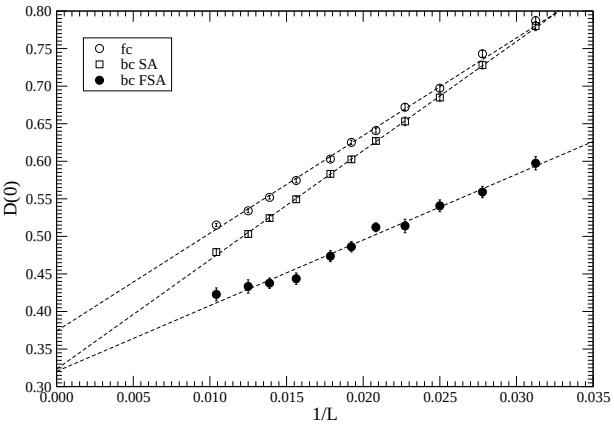

FIG. 2: $D(0)$ as a function of L for *fc* (the same for SA and FSA), *bc* SA (without flips) and *bc* FSA.

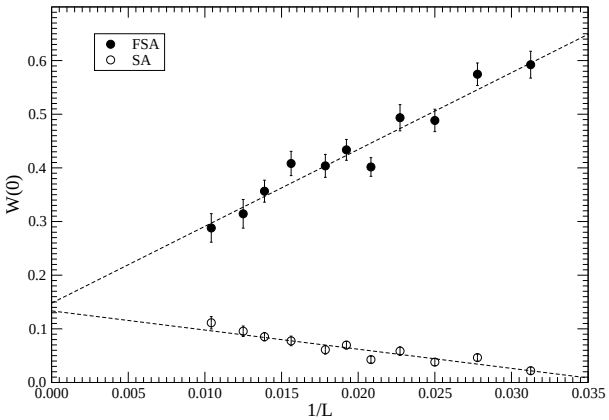

FIG. 3: $W(0)$ as a function of L for FSA and SA.

V. CONCLUSIONS

In this work we investigated numerically the Landau gauge gluon propagator $D(p)$ in the three-dimensional pure gauge $SU(2)$ lattice theory. The main goal was to study the approach of the zero-momentum propagator $D(0)$ to the thermodynamic limit $L \to \infty$. We have employed eleven lattice volumes from $L = 32$ to $L = 96$. All calculations have been made at $\beta = 4.24$ ($a = 0.168$ fm).

Special attention in this study has been paid to the dependence on the choice of Gribov copies. To this purpose we have generated up to 280 gauge copies for every configuration. Our *bc* FSA method provides systematically higher values of the gauge fixing func-

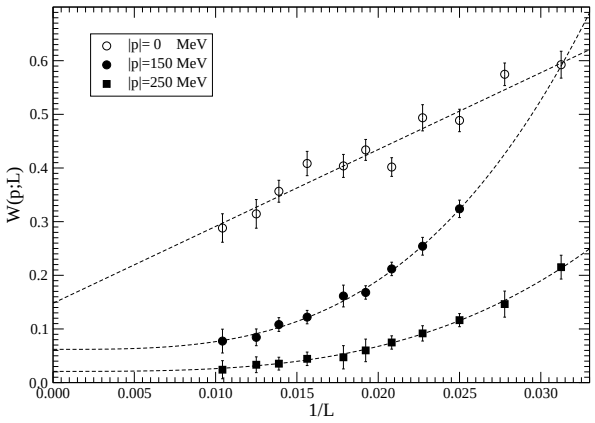

FIG. 4: $W(p)$ as a function of L for FSA for three different values of $|p|$.

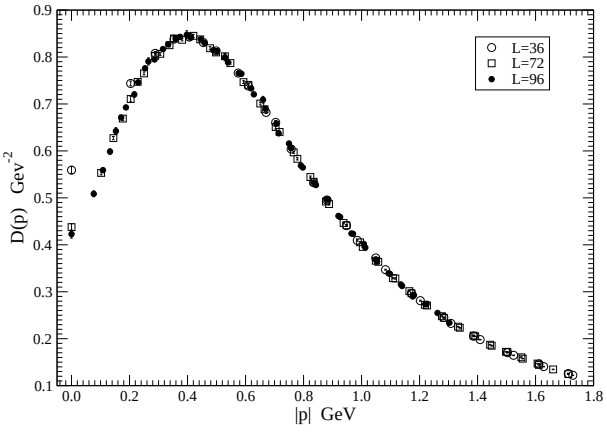

FIG. 5: The momentum dependence of $D(p)$ for **three lattices.**

tional as compared to the *fc* FSA and *bc* SA methods.

The main results are the following.

1. In the limit $L \to \infty$ the value of $D(0; L)$ differs from zero (in agreement with [28]).

2. The Gribov copy influence is very strong in the deep infrared region (especially for $D(0)$), and by no means can be considered as a "Gribov noise".

Moreover, our analysis shows that the Gribov copy effects remain substantial (up to $\sim 15\%$ for zero-momentum propagator) even in the thermodynamic limit $L \to \infty$. The choice of the efficient gauge fixing procedure is of crucial importance in this study.

3. The finite-volume effects for the gluon propagator at momenta greater than 400 MeV are negligibly small.

Acknowledgments

This investigation has been partly supported by the Heisenberg-Landau program of collaboration between the Bogoliubov Laboratory of Theoretical Physics of the Joint Institute for Nuclear Research Dubna (Russia) and German institutes, by the joint DFG-RFBR grant 436 RUS 113/866/0-1 and the RFBR-DFG grant 11-02-91339-NNIOa, by the Federal Special-Purpose Programme "Cadres" of the Russian Ministry of Science and Education. VB is supported by grant RFBR 11-02-01227-a.

[1] V. N. Gribov, Nucl. Phys. **B139**, 1 (1978).
[2] D. Zwanziger, Nucl. Phys. **B364**, 127 (1991).
[3] D. Dudal, S. P. Sorella, N. Vandersickel, and H. Verschelde, Phys. Rev. **D77**, 071501 (2008), 0711.4496.
[4] D. Dudal, J. A. Gracey, S. P. Sorella, N. Vandersickel, and H. Verschelde, Phys. Rev. **D78**, 065047 (2008), 0806.4348.
[5] D. Dudal, J. A. Gracey, S. P. Sorella, N. Vandersickel, and H. Verschelde, Phys. Rev. **D78**, 125012 (2008), 0808.0893.
[6] L. von Smekal, R. Alkofer, and A. Hauck, Phys. Rev. Lett. **79**, 3591 (1997), hep-ph/9705242.
[7] R. Alkofer and L. von Smekal, Phys. Rept. **353**, 281 (2001), hep-ph/0007355.
[8] J. M. Cornwall, Phys.Rev. **D26**, 1453 (1982).
[9] C. S. Fischer, A. Maas, and J. M. Pawlowski, Annals Phys. **324**, 2408 (2009), 0810.1987.
[10] A. C. Aguilar, D. Binosi, and J. Papavassiliou, Phys. Rev. **D78**, 025010 (2008), 0802.1870.
[11] P. Boucaud et al., JHEP **06**, 012 (2008), 0801.2721.
[12] M. A. Semenov-tyanShanskii and V. A. Franke, *Zapiski Nauch. Sem. Leningradskogo otd. Matematicheskiogo inst. im. V.A.Steklova* **120**, 159 (1982), translation: (Plenum, NY, 1986) p.199.
[13] C. Parrinello and G. Jona-Lasinio, Phys. Lett. **B251**, 175 (1990).

[14] D. Zwanziger, Nucl. Phys. **B345**, 461 (1990).

[15] A. Nakamura and M. Plewnia, Phys. Lett. **B255**, 274 (1991).

[16] V. G. Bornyakov, V. K. Mitrjushkin, M. Müller-Preussker, and F. Pahl, Phys. Lett. **B317**, 596 (1993), hep-lat/9307010.

[17] V. K. Mitrjushkin, Phys. Lett. **B389**, 713 (1996), hep-lat/9607069.

[18] I. L. Bogolubsky, G. Burgio, V. K. Mitrjushkin, and M. Müller-Preussker, Phys. Rev. **D74**, 034503 (2006), hep-lat/0511056.

[19] I. L. Bogolubsky, V. G. Bornyakov, G. Burgio, E.-M. Ilgenfritz, V. K. Mitrjushkin, and M. Müller-Preussker, Phys. Rev. **D77**, 014504 (2008), 0707.3611.

[20] V. G. Bornyakov, V. K. Mitrjushkin, and M. Müller-Preussker, Phys. Rev. **D79**, 074504 (2009), 0812.2761.

[21] V. Bornyakov, V. Mitrjushkin, and M. Muller-Preussker, Phys.Rev. **D81**, 054503 (2010), 0912.4475.

[22] V. Bornyakov and V. Mitrjushkin, Phys.Rev. **D84**, 094503 (2011), 1011.4790.

[23] I. L. Bogolubsky, E.-M. Ilgenfritz, M. Müller-Preussker, and A. Sternbeck, Phys. Lett. **B676**, 69 (2009), 0901.0736.

[24] R. Aouane, V. Bornyakov, E.-M. Ilgenfritz, V. Mitrjushkin, M. Muller-Preussker, et al. (2011), 1108.1735.

[25] V. Bornyakov and V. Mitrjushkin (2011), 1103.0442.

[26] A. Cucchieri, T. Mendes, and A. R. Taurines, Phys. Rev. **D67**, 091502 (2003), hep-lat/0302022.

[27] A. Cucchieri, T. Mendes, and A. R. Taurines, Phys. Rev. **D71**, 051902 (2005), hep-lat/0406020.

[28] A. Cucchieri and T. Mendes, PoS **LAT2007**, 297 (2007), 0710.0412.

[29] A. Cucchieri, A. Maas, and T. Mendes, Phys. Rev. **D75**, 076003 (2007), hep-lat/0702022.

[30] A. Maas, Phys. Rev. **D79**, 014505 (2009), 0808.3047.

[31] A. Cucchieri, D. Dudal, T. Mendes, and N. Vandersickel (2011), 1111.2327.

[32] J. E. Mandula and M. Ogilvie, Phys. Lett. **B185**, 127 (1987).

[33] P. Schemel, Diploma thesis, Humboldt University Berlin/Germany (2006).

[34] I. L. Bogolubsky, V. G. Bornyakov, G. Burgio, E.-M. Ilgenfritz, V. K. Mitrjushkin, M. Müller-Preussker, and P. Schemel, PoS **LAT2007**, 318 (2007), 0710.3234.

[35] M. J. Teper, Phys.Rev. **D59**, 014512 (1999), hep-lat/9804008.

[36] D. Zwanziger, Phys. Rev. **D69**, 016002 (2004), hep-ph/0303028.

[37] A. Maas, A. Cucchieri, and T. Mendes (2006), hep-lat/0610006.